

# Numerical Investigation of the Effect of Aluminum Yielding Damper for the Retrofitting of Semi-rigid Steel Frames

Hamidreza Aghani<sup>1</sup>, Kambiz Cheraghi<sup>2\*</sup>, Mohammad Bakhshipour<sup>1</sup>

<sup>1</sup> Department of Civil engineering, Kermanshah Branch, Islamic Azad University, Kermanshah 6714414971, Iran

<sup>2</sup> Department of Civil Engineering, Faculty of Engineering, Razi University, Kermanshah 6714473421, Iran

\* Corresponding author, e-mail: [kambiz.cheraghi@gmail.com](mailto:kambiz.cheraghi@gmail.com)

Received: 03 August 2023, Accepted: 28 September 2023, Published online: 19 October 2023

## Abstract

During an earthquake, yielding dampers yield before the main members of the structure and with their plastic deformations, they dissipate part of the earthquake energy. Therefore, ductile materials are a suitable option for this type of dampers. In this research, numerical studies were conducted to investigate the effect of aluminum yielding damper (AYD) on semi-rigid steel frame. First, the steel frame and the AYD were verified based on experimental samples and analytical equations. An approximate equation for estimating the elastic stiffness of the damper was also presented. Parametric studies were conducted in order to investigate the effect of the number of dampers and the axial force of the column on the stiffness, ultimate strength, ductility and energy dissipation parameters of the frame. The additional forces applied to the connections, beams and columns of the frame due to the addition of dampers were also calculated, which is important in the design of the frame. The results showed that the addition of the damper increased the frame's stiffness, energy dissipation, ultimate strength, and ductility, and also reduced the negative effect of the column's axial force on energy dissipation of the frame.

## Keywords

aluminum yielding damper, energy dissipation, semi-rigid steel frame, numerical analysis

## 1 Introduction

Earthquakes pose a significant threat to structures, causing damage and failure. Despite technological advancements, accurately predicting earthquake events remains a challenge. To mitigate the destructive effects of earthquake loads, numerous vibration control systems have been proposed [1–3]. These systems can be broadly categorized as passive, active, semi-active, and hybrid [4–6]. Among these, passive control systems, such as metallic dampers, offer substantial damping capacity without requiring external energy sources. Metallic dampers have advantages such as high efficiency, rate independence, and resistance to ambient temperature, making them cost-effective and appealing for mitigating seismic forces on structures [7]. Semi-rigid frames are one of the laterally resistant systems that have high ductility but have little stiffness and lateral resistance [8, 9].

Until now, different geometries of yielding dampers have been used to strengthen concrete and steel structures. Farsi et al. [10] proposed a C-Shaped Damper (CSD) for braced frame structures. The CSD dissipates earthquake

energy using sacrificial C-Shaped elements, protecting main structural elements. Parametric investigations showed the CSD's yielding force was influenced by its dimensions, and it exhibited suitable energy dissipation and replaceability after failure. Houshmand-Sarvestani et al. [11] studied the effects of steel-plate added damping and stiffness (ADAS) dampers on steel shear walls (SSWs). The results showed that ADAS dampers improved seismic behavior, increased damping capability, and enhanced ductility in SSWs. Akbari Hamed et al. [12] developed multi-level TADAS dampers to protect structural and non-structural components during minor and major earthquakes. The dampers showed improved seismic performance, with structures equipped with them exhibiting higher yield and collapse points compared to those without dampers. Additionally, these dampers make it possible for the design of lightweight structures, supporting sustainable development goals. TahamouliRoudsari et al. [13] investigated the effects of TADAS damper and column axial force on the stiffness, strength, and ductility of a scaled

RC frame. Results showed that a three-fold increase in shear capacity led to the best response, while an axial force above 0.2 Pcr reduced energy dissipation and ductility. Ghalehnavi et al. [14] studied the effect of rotational, viscous, and TADAS frictional dampers on an 8-story steel frame structure. The results showed that damper specifications should be based on individual floor behavior rather than the overall structure. Ghaedi et al. [7] investigated the effectiveness of an innovative metallic damper, the bar damper, in enhancing the cyclic performance of a semi-rigid frame. Experimental tests and finite element models demonstrated that the bar damper devices significantly improved the frame's strength, stiffness, damping ratio, and energy dissipation capacity. Rai et al. [15] conducted a shake table study comparing conventional braced frames (OCBF) to aluminum shear-link enabled frames (SLBF). SLBF exhibited lower base shear, overturning moments, and floor acceleration. Aluminum shear-links absorbed significant energy, enabling SLBF to withstand higher seismic loads. Ferraioli et al. [16] developed a design method for seismic retrofitting of reinforced concrete buildings using aluminum multi-stiffened shear panels as dampers. The method considers nonlinearity in the structure and dampers-structure interaction to optimize panel distribution. The proposed procedure was validated through analysis of two RC buildings, demonstrating its effectiveness in reducing inter-story drift and avoiding weak story collapse. Yadav and Sahoo [17] developed an innovative energy dissipation device called the sandwiched shear yielding plate (SSYP). Experimental tests showed stable hysteretic response and high energy dissipation capacity. Analytical expressions and a simplified macro model were proposed for design and numerical modeling of the SSYP.

In many past researches, the placement of yielding dampers has been proposed as shown in Fig. 1(a), which shows the state before and after lateral loading. It can be seen that the displacement of the damper and the steel frame are the same Fig. 1(b). Therefore, according to the law of springs, the lateral force is divided between them according to the stiffness of the frame and the stiffness of the damper, in the form of Eqs. (1) and (2). In these equations,  $k_f$  and  $k_d$  represent the lateral stiffness of the frame and the displacement of the spring (or yielding damper), respectively. Similarly, the stiffness ratio of these two members is essential in damper design.

$$F_d = \frac{K_d}{K_f + K_d} F \tag{1}$$

$$F_f = \frac{K_f}{K_f + K_d} F \tag{2}$$

## 2 Verification of the numerical model

### 2.1 Verification of semi-rigid steel frame

To verify the semi-rigid steel frame, Hsu and Halim [18] experimental sample was used. The schematic model of this sample is depicted in Fig. 2. This frame was laterally loaded. Also, the connection of the column to the ground in this frame is designed as a hinge.

Modeling of the experimental frame was done using shell element (S4R) in ABAQUS software. The analysis of the model was done using the Static General solver. In the numerical model, large deformations were also considered. The material used for the steel frame is known as ST37. Its stress-strain curve is described below. Also, the model analysis was done using displacement-control technique.

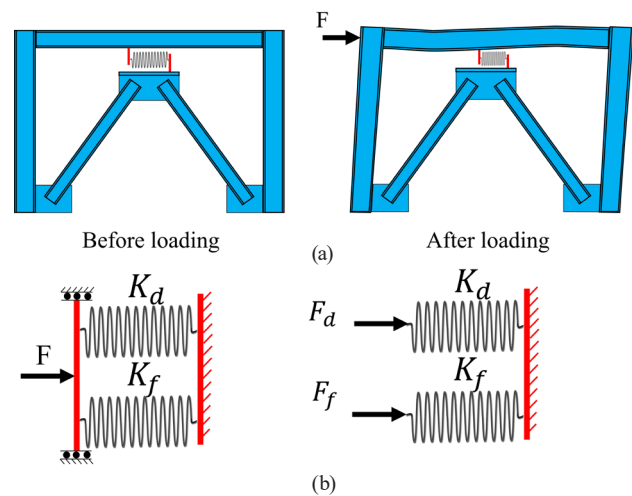


Fig. 1 (a) Frame equipped with damper before and after loading, (b) distribution of force between members

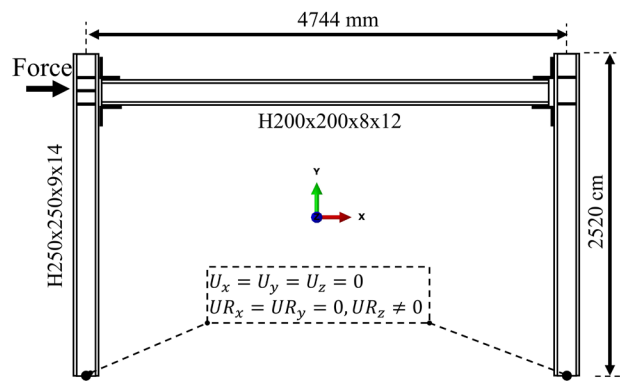


Fig. 2 Dimensions and characteristics of the experimental sample

The dimensions of the mesh of the frame and its stiffeners were considered equal to 20 mm (Fig. 3(a)) according to the sensitivity analysis. Fig. 3(b) shows the von Mises stress contour of the frame at a displacement of 120 mm. After analyzing the frame, the force-displacement diagram of the frame was compared with the results of the experimental result in Fig. 4. It can be seen that the numerical model is reasonably close to the experimental results.

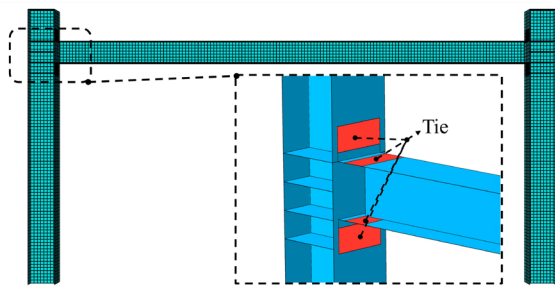
### 2.2 Verification of AYD

In this section, the numerical model of AYD was verified with analytical equations. Damper geometry was considered as Fig. 5(a). The material used for this damper was defined as aluminum, following the research by De Matteis, et al. [19], and its stress-strain behavior is depicted in Fig. 6.

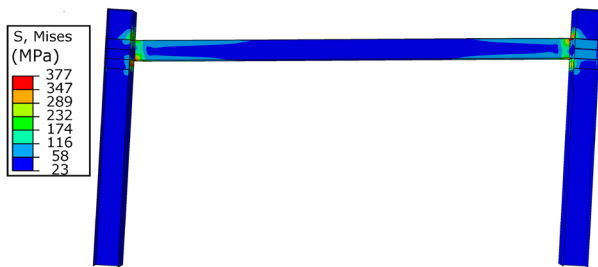
The stiffness of the damper can be determined using Castigliano's theorem [20], as given in Eq. (3), where the moment of inertia for different sections is considered based

on Eq. (4). These equations are applicable to Fig. 5(a). To expedite the estimation of the damper's stiffness, an approximate equation, Eq. (5), was derived using curve fitting techniques. The comparison results of the elastic stiffness obtained from the exact Eq. (3) and the approximate Eq. (5) for various modes of the damper are presented in Table 1. The table demonstrates that the approximate equation closely aligns with the exact results.

If the damper is subjected to a lateral load, the yield force is equivalent to the force that causes the formation of a plastic hinge as shown in Fig. 5(b). This force can be calculated according to Eq. (6), where  $\sigma_y$  is the yield stress of aluminum, which is reported to be 20 MPa [19].



(a)



(b)

Fig. 3 (a) Numerical model meshing, (b) Stress contour of the model after loading

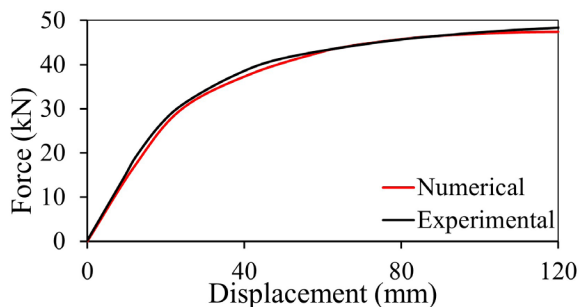


Fig. 4 Comparison of numerical and experimental model results [18]

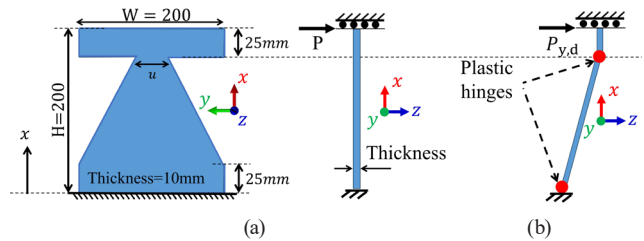


Fig. 5 (a) The dimensions of the AYD (b) damper yielding mechanism

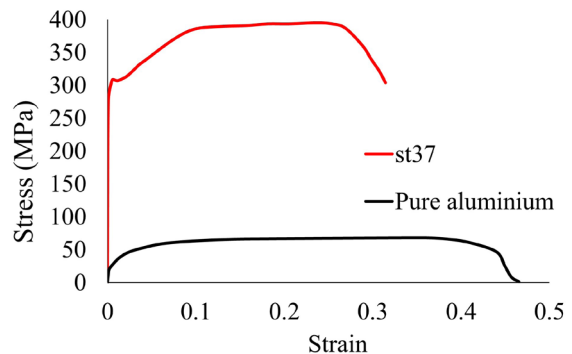


Fig. 6 Strain stress for ST37 and aluminum [19]

Table 1 Comparing damper stiffness results from exact and approximate methods

Dimensions of the AYD (mm)			Elastic stiffness (kN/mm)		Error (%)
<i>W</i>	<i>H</i>	<i>u</i>	Exact Eq. (3)	App. Eq. (5)	
150	150	30	1.99	2.02	1.5
175	225	105	0.95	0.95	0.0
175	250	140	0.75	0.75	0.0
200	200	40	1.12	1.14	1.8
200	225	40	0.79	0.80	1.3
250	200	175	2.02	2.02	0.0
150	250	30	0.43	0.44	1.3
175	175	52.5	1.67	1.66	0.6
250	250	200	1.07	1.07	0.0

$$K_{e,d} = P / \int \frac{M}{EI_i} \frac{\partial M}{\partial P} dx \quad (i = 1, 2, 3) \quad (3)$$

$$I_2 = \left( \frac{(u-W)x}{150} - \frac{7W-u}{6} \right) \times \frac{10^3}{12} \quad 25 < x < 175 \quad (4)$$

$$I_1 = 200 \times \frac{10^3}{12} \quad 0 < x < 25$$

$$I_3 = 200 \times \frac{10^3}{12} \quad 175 < x < 200$$

$$K_{e,d,app} = 71435.3 \times W^{0.72} \times \frac{u^{0.28}}{H^3} \quad (kN / mm) \quad (5)$$

$$P_{y,d} = \frac{(W+u)t^2}{3H} \sigma_{y,d} \quad (6)$$

Numerical model of AYD using shell element (S4R) was done as shown in Fig. 7. All assumptions considered for this model were made similar to steel frame modeling. To verify the results of the numerical model, the damper with the dimensions shown in Fig. 5 was analyzed with variable  $u$  and its results are shown in Fig. 8(a). Then, its elastic stiffness and yield strength were compared with Eqs. (3) and (6), which are shown in Figs. 8(b) and 8(c), respectively. It can be seen that the results are close to each other with acceptable accuracy.

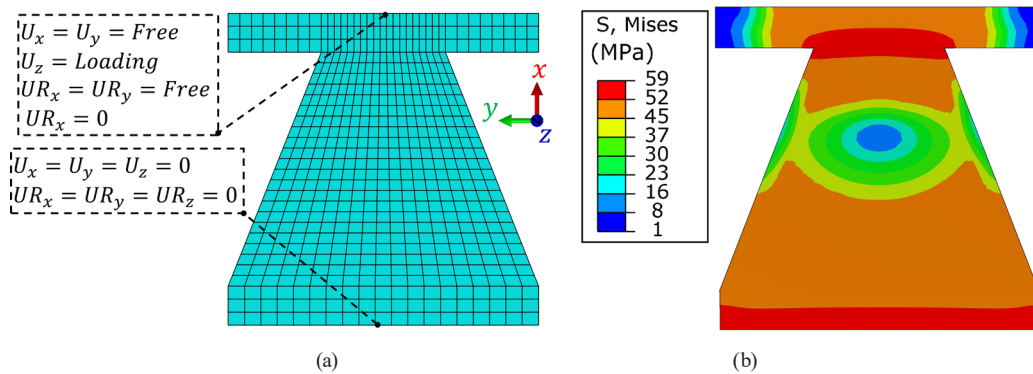


Fig. 7 (a) Boundary conditions of the numerical model (b) Stress contour of the AYD at the final moment

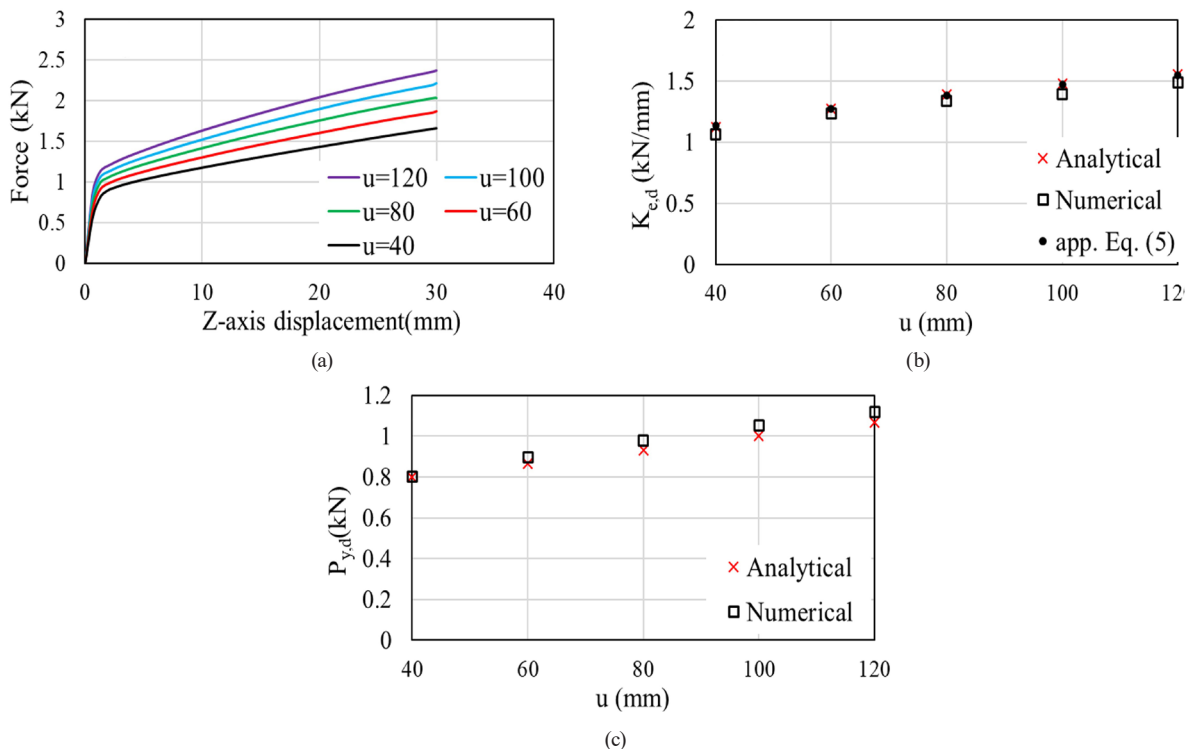


Fig. 8 (a) The numerical results of the model shown in Fig. 5(a) Comparison of numerical and analytical results of (b) elastic stiffness and (c) yield strength

### 3 Parametric study

In this section, a semi-rigid steel frame equipped with a yield damper is investigated. The parametric model examined here is shown in Fig. 9. The location of the damper is based on suggestions from previous research [21–24]. The braces in this model are designed not to buckle until the end of loading in any of the models. To model the brace members and connecting plates, the shell element (S4R) is utilized. Additionally, the connection between the members of the model is accomplished with a "Tie" constraint. The analysis of the models is performed using the displacement-control technique, and the loading continued until the point of curve drop. The steel frame and damper with dimensions and specifications similar to the approved model were considered in this section.

All the models analyzed in this section are listed in Table 2. As can be seen, the variables of the parametric model include the number of dampers and the axial force of the column. The stiffness of the semi-rigid frame is reported to be 1.48 kN/mm [18]. The axial force of the column was also applied as a percentage of its critical load. The critical load of the column was calculated as 1860kN

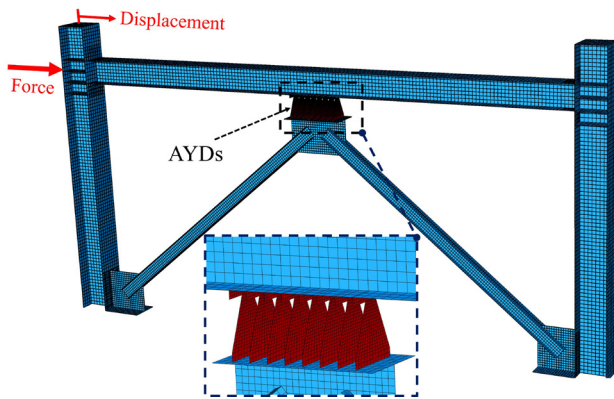


Fig. 9 Semi-rigid steel frame equipped with AYDs

according to AISC 360-16 [25]. As can be seen, the naming of the models is based on the ratio of lateral stiffness of the damper to the frame and the ratio of the axial load to the critical load of the column.

After obtaining the force-displacement diagrams for the models listed in Table 2, their simplified bilinear diagrams were calculated following the guidelines from FEMA [26]. According to this code, the equivalent bilinear diagram should be determined such that the area under both diagrams is equal, and both curves intersect at 0.6 of the yield force. The schematic of the non-linear and bilinear diagrams can be observed in Fig. 10. The horizontal and vertical axes in this figure represent lateral displacement and lateral force, which are shown in Fig. 9.

Fig. 11 provides four examples of the results obtained for the models presented in Table 2, along with their respective bilinear diagrams. Additionally, using Eqs. (7) and (8), the lateral stiffness of the frame and ductility can be calculated, respectively. Moreover, the energy dissipation is defined as the area under the curve.

$$K_{e,f} = V_y / D_y \tag{7}$$

$$Ductility = D_u / D_y \tag{8}$$

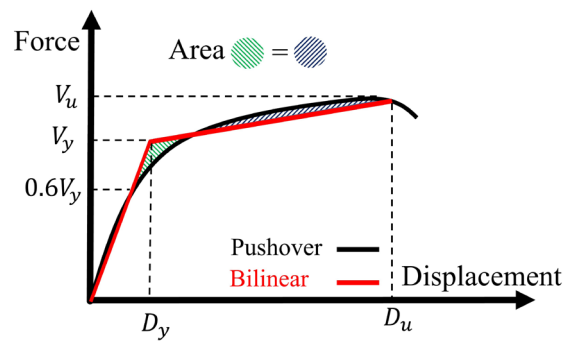


Fig. 10 Non-linear curve and bilinear equivalent

Table 2 Specifications of parametric models

Model	Dimensions of the AYD (mm)		No. of AYD	$\alpha = \frac{K_{e,d}}{K_{e,frame}}$	$\beta = \frac{P}{P_{cr}}$
	$W = H$	$u$			
SF-0-0, SF-0-0.2, SF-0-0.4	200	60	0	0	0, 0.2, 0.4
SF-0.87-0, SF-0.87-0.2, SF-0.87-0.4			1	0.87	
SF-1.73-0, SF-1.73-0.2, SF-1.73-0.4			2	1.73	
SF-2.59-0, SF-2.59-0.2, SF-2.59-0.4			3	2.59	
SF-3.45-0, SF-3.45-0.2, SF-3.45-0.4			4	3.45	
SF-4.31-0, SF-4.31-0.2, SF-4.31-0.4			5	4.31	
SF-5.18-0, SF-5.18-0.2, SF-5.18-0.4			6	5.18	
SF-6.04-0, SF-6.04-0.2, SF-6.04-0.4			7	6.04	
SF-6.90-0, SF-6.90-0.2, SF-6.90-0.4			8	6.90	

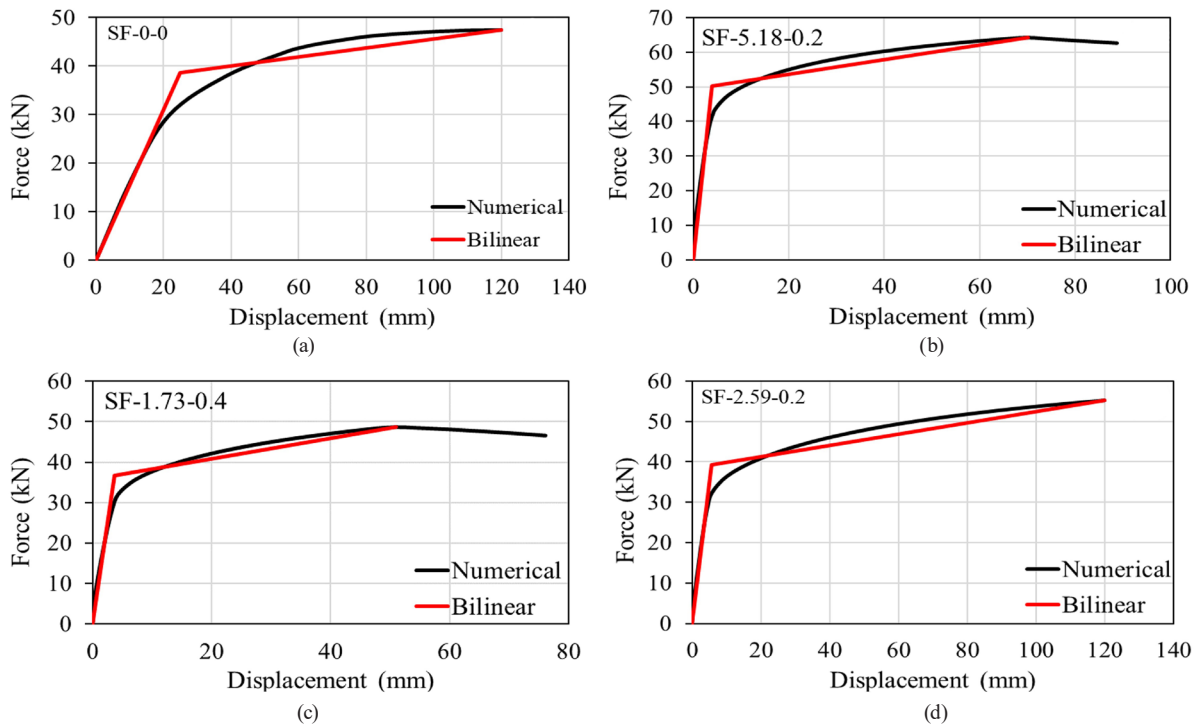


Fig. 11 The results of the numerical models introduced in Table 2 and their bilinear diagrams for (a)SF-0-0, (b) SF-5.18-0.2, (c) SF-1.73-0.4, (d) SF-2.59-0.2

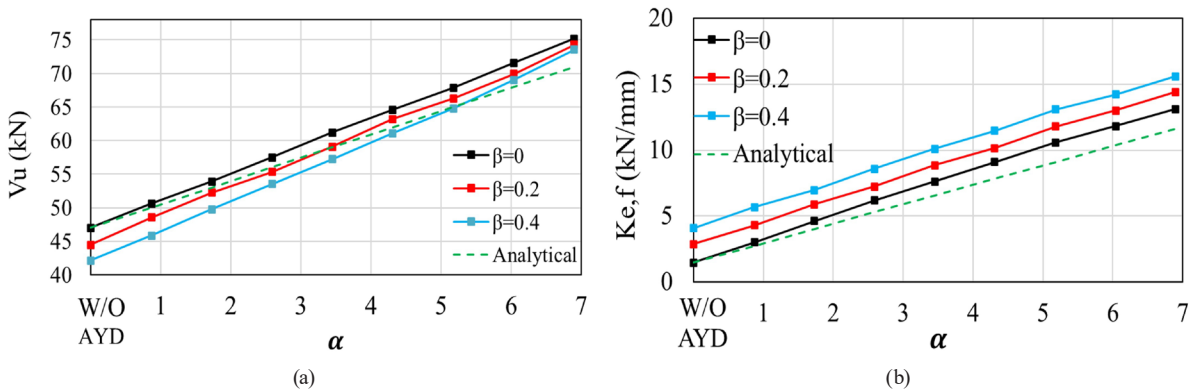


Fig. 12 The results of the (a) ultimate strength and (b) stiffness of the frame equipped with AYDs

After extracting all the force-displacement diagrams of the models in Table 2, in this section, the parameters calculated from these curves, including elastic stiffness, ultimate strength ( $V_u$ ), energy dissipation (ED) and ductility, were examined. Figs. 12(a) and 12(b) show the ultimate strength and elastic stiffness of the steel frame equipped with AYDs, respectively. It can be observed that the rate of increase of these two parameters with respect to  $\alpha$  (the stiffness ratio of the AYDs to the bare steel frame) was nearly linear. Additionally, the axial force has a reducing effect on the ultimate strength while increasing the stiffness of the frame.

According to Fig. 1, it can be seen that the dampers and the steel frame are parallel springs, as they have the same displacement. Thus, the ultimate strength and stiffness of

the frame can be expressed using Eqs. (9) and (10), where 'n' represents the number of dampers used in the frame, and denotes the ultimate stress of the damper, which is equal to 69 MPa [18]. Figs. 12(a) and 12(b) also present the results of these equations alongside the numerical findings.

$$V_u = V_{u,original\ frame} + n \frac{(W + u)t^2}{3H} \sigma_{u,d} \tag{9}$$

$$K_{e,f} = K_{e,original\ frame} + n K_{e,d} \tag{10}$$

Figs. 13(a) and 13(b) show the normalized ductility and energy dissipation compared to the original frame (without axial load). In these figures, the vertical axes display the results of the models in comparison to the SF-0-0 model. It can be observed that the curves' slope in both results was

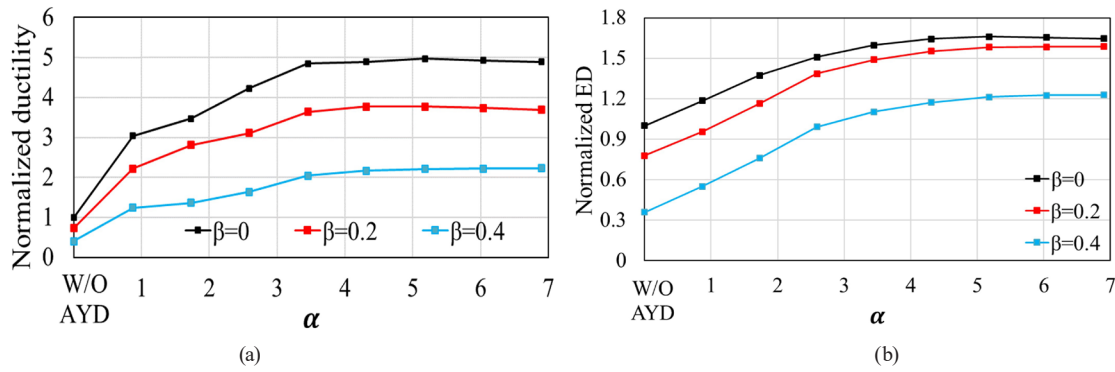


Fig. 13 Normalized results related to (a) ductility, (b) energy dissipation

step before  $\alpha = 3.45$ , and after that, it remained almost constant. Additionally, both results show that the axial force has a reducing effect on the results, but this negative influence diminishes with the increase of the AYDs in the frame. Notably, the models with a critical axial force of 0.4 Pcr ( $\beta = 0.4$ ) and  $\alpha$  equal to 6.9 demonstrate higher ductility and energy dissipation compared to the original frame (frame without damper) without axial force.

#### 4 Investigation of steel frame stresses

In this section, the Van Mises stress of the semi-rigid frame model equipped with a damper has been investigated. Since the final yield mechanism of all models was almost the same, the stress contour of model SF-2.59-0.2 is presented as an example. Fig. 14 shows the von Mises stress contour of the model at the moment of drop of the force-displacement diagram. It can be seen that the beam has yielded in the connection areas. Additionally, the AYD is also yielded at both ends.

#### 5 Forces applied to the frame after damper addition

With the addition of AYDs to the semi-rigid steel frame, additional forces are applied to the connections, columns, and beams, which are discussed in this section. The schematic model of the frame and the forces applied to it are shown in Fig. 15(a). AYDs apply concentrated moments to the beam, which can be considered as concentrated due to the small length  $L_d$ . Additionally, frame connections can be considered as concentrated springs. Consequently, its free diagram will be in the form of Fig. 15(b). Given that problem Fig. 15(b) represents an indeterminate beam, the force method [20] was employed for its analysis. Similarly, the axial force within the column and its connection moments were calculated as Eqs. (11) to (13). The maximum moment of the beam can also be calculated according to Eq. (14).

For a quicker estimation of the maximum beam moment, contour Fig. 16 was provided, allowing the calculation of the maximum beam moment using  $x$  and  $\varphi$  values.

$$F_{column} = \frac{6M_d(\varphi x + 1 - \varphi x^2)}{(\varphi + 6)L} \quad (11)$$

$$M_{c1} = M_d \times \varphi \left( \frac{2\varphi x - 3\varphi x^2 + 2 - 6x^2}{\varphi^2 + 8\varphi + 12} \right) \quad (12)$$

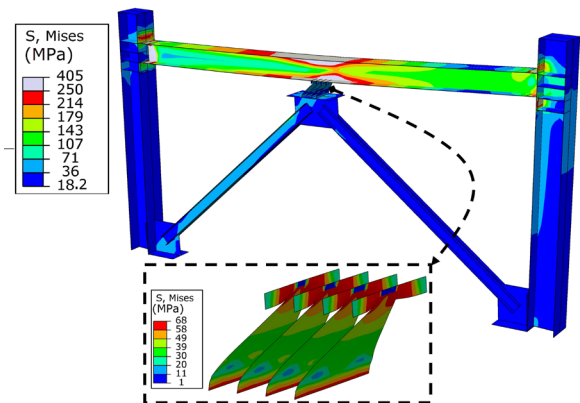


Fig. 14 Van Mises stress contour model SF-2.59-0.2

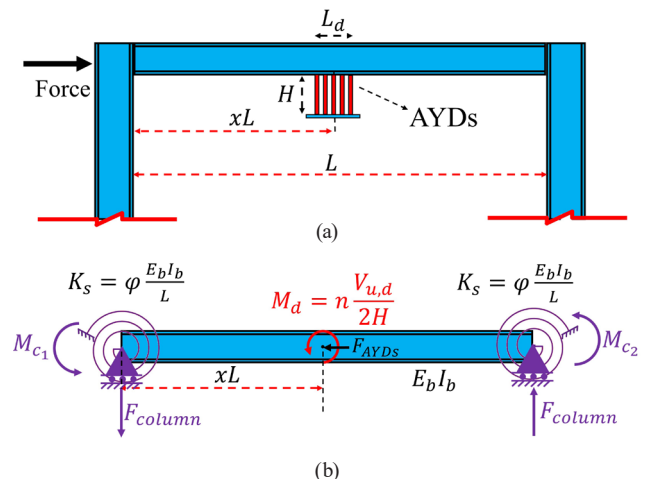


Fig. 15 (a) Schematic of the forces applied to the frame, (b) Free body diagram of the beam

$$M_{c_2} = F_{column}L - M_d \left( 1 + \varphi \left( \frac{2\varphi x - 3\varphi x^2 + 2 - 6x^2}{\varphi^2 + 8\varphi + 12} \right) \right) \quad (13)$$

$$M_{\max(\text{beam})} = \max \left( \begin{array}{l} F_{column}(1-x)L - M_{c_2} \\ M_d - F_{column}(1-x)L - M_{c_2} \end{array} \right) \quad (14)$$

## 6 Conclusions

Parametric studies were conducted in this research to explore the impact of the yielding damper on the semi-rigid frame. The analysis of the models was performed using non-linear static method. The variables in the parametric model included the column axial force and the number of AYDs in the frame. Initially, the semi-rigid steel frame and damper were verified using experimental samples and analytical relationships, respectively. The analyses conducted in this study were executed on a one-story, one-span semi-rigid steel frame using the displacement control method. Subsequently, the frame's stiffness, ultimate strength, energy dissipation, and ductility were examined. Additionally, the additional forces exerted on the frame due to the damper were calculated. The results were summarized as follows:

- The axial force reduced the energy dissipation, ductility, ultimate strength of the frame, and increased the lateral stiffness.
- The ratio of the elastic stiffness of the damper to the stiffness of the frame is one of the crucial factors influencing the behavior of semi-rigid steel frames equipped with AYD. An approximate equation was also presented that makes it possible to estimate the damper's stiffness with acceptable accuracy.

## References

- [1] TahamouliRoudsari, M., Cheraghi, K., Habibi, M. R. "Investigation of retrofitting RC moment resisting frames with ADAS yielding dampers", *Asian Journal of Civil Engineering*, 20, pp. 125–133, 2019. <https://doi.org/10.1007/s42107-018-0092-6>
- [2] Cheraghi, K., Tavana, M. H., Aghayari, R. "Investigating the Effect of Low-Yield Yielding Dampers on the Seismic Behavior of Steel Frames", *Periodica Polytechnica Civil Engineering*, 2023. <https://doi.org/10.3311/PPci.21804>
- [3] Cheraghi, K., TahamouliRoudsari, M., Kiasat, S. "Numerical and analytical investigation of U-shape dampers and its effect on steel frames", *Structures*, 55, pp. 498–509, 2023. <https://doi.org/10.1016/j.istruc.2023.06.037>
- [4] Wang, L., Nagarajaiah, S., Shi, W., Zhou, Y. "Seismic performance improvement of base-isolated structures using a semi-active tuned mass damper", *Engineering Structures*, 271, 114963, 2022. <https://doi.org/10.1016/j.engstruct.2022.114963>
- [5] Feng, Y., Liu, W., Xu, H., Zhang, Q. "Theoretical study and experimental verification on a passive control system with isolators and dampers for NPPs", *Journal of Building Engineering*, 60, 105195, 2022. <https://doi.org/10.1016/j.job.2022.105195>
- [6] Cao, L., Li, C. "A high performance hybrid passive base-isolated system", *Structural Control and Health Monitoring*, 29, e2887, 2022. <https://doi.org/10.1002/stc.2887>
- [7] Ghaedi, K., Javanmardi, A., Ibrahim, Z., Gordan, M., Rashid, R. S. M., Khatibi, H., Vaghei, R. "Experimental and numerical studies on the cyclic performance of structural frames equipped with bar dampers", *Structures*, 50, pp. 707–722, 2023. <https://doi.org/10.1016/j.istruc.2023.02.070>
- [8] Csébfalvi, A. "Optimal design of frame structures with semi-rigid joints", *Periodica Polytechnica Civil Engineering*, 51(1), pp. 9–15, 2007. <https://doi.org/10.3311/pp.ci.2007-1.02>

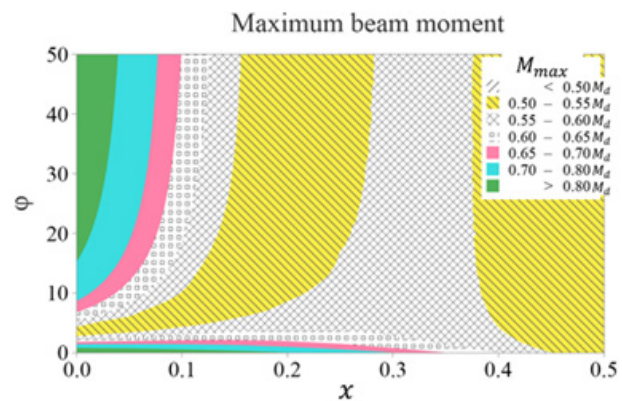


Fig. 16 The maximum moment of the beam relative to the value of  $x$  and  $\varphi$

- The increase in lateral stiffness and ultimate strength of the frame showed an almost linear correlation with the increase in  $\alpha$  (the ratio of the elastic stiffness of the damper to the original frame).
- By increasing the number of AYDs in the frame, the energy dissipation and ductility of the frame increased. The rate of increase was steep until the  $\alpha$  value reached 3.45, after which it became almost constant. Additionally, adding more dampers lessened the negative impact of the axial force on the energy dissipation.
- The addition of the damper to the frame resulted in additional forces applied to various frame components, including connections, beams, and columns. Equations were presented to calculate the forces applied to these parts, which can be considered in designing the frame.

- [9] Papp, F. "Parametric Study on the Influence of Semi-Rigid Frame Knees and Support Conditions", *Periodica Polytechnica Civil Engineering*, 41(1), pp. 29–50, 1997.
- [10] Farsi, A., Amiri, H. R., Dehghan Manshadi, S. H. "An innovative C-shaped yielding metallic dampers for steel structures", *Structures*, 34, pp. 4254–4268, 2021.  
<https://doi.org/10.1016/j.istruc.2021.08.069>
- [11] Houshmand-Sarvestani, A., Totonchi, A., Shahmohammadi, M. A., Salehipour, H. "Numerical assessment of the effects of ADAS yielding metallic dampers on the structural behavior of steel shear walls (SSWs)", *Mechanics Based Design of Structures and Machines*, 51(3), pp. 1626–1644, 2023.  
<https://doi.org/10.1080/15397734.2021.1875328>
- [12] Akbari Hamed, A., Mortazavi, S. F., Saeidzadeh, M. "Evaluation of the seismic performance of structures equipped with novel multi-level TADAS dampers", *Asian Journal of Civil Engineering*, 24(4), pp. 969–988, 2023.  
<https://doi.org/10.1007/s42107-022-00546-5>
- [13] TahamouliRoudsari, M., Cheraghi, K., Aghayari, R. "Investigating the Retrofit of RC Frames Using TADAS Yielding Dampers", *Structural Durability & Health Monitoring*, 16(4), pp. 343–359, 2022.  
<https://doi.org/10.32604/sdhm.2022.07927>
- [14] Ghalehnovi, M., Karimipour, A., Azad Darmian, J. "Study of the effect of friction rotational damper, viscoelastic and TADAS on the structures seismic behaviour", *Journal of Modeling in Engineering*, 17(59), pp. 87–107, 2019.  
<https://doi.org/10.22075/jme.2019.14484.1433>
- [15] Rai, D. C., Annam, P. K., Pradhan, T. "Seismic testing of steel braced frames with aluminum shear yielding dampers", *Engineering Structures*, 46, pp. 737–747, 2013.  
<https://doi.org/10.1016/j.engstruct.2012.08.027>
- [16] Ferraioli, M., Lavino, A., De Matteis, G. "A design method for seismic retrofit of reinforced concrete frame buildings using aluminum shear panels", *Archives of Civil and Mechanical Engineering*, 23(2), 106, 2023.  
<https://doi.org/10.1007/s43452-023-00639-1>
- [17] Yadav, D., Sahoo, D. R. "Experimental and analytical investigations of buckling-inhibited aluminum shear yielding devices under cyclic loading", *Soil Dynamics and Earthquake Engineering*, 172, 108007, 2023.  
<https://doi.org/10.1016/j.soildyn.2023.108007>
- [18] Hsu, H.-L., Halim, H. "Brace performance with steel curved dampers and amplified deformation mechanisms", *Engineering Structures*, 175, pp. 628–644, 2018.  
<https://doi.org/10.1016/j.engstruct.2018.08.052>
- [19] De Matteis, G., Formisano, A., Panico, S., Mazzolani, F. M. "Numerical and experimental analysis of pure aluminium shear panels with welded stiffeners", *Computers & Structures*, 86(6), pp. 545–555, 2008.  
<https://doi.org/10.1016/j.compstruc.2007.05.027>
- [20] Hibbeler, R. C. "Structural analysis", Pearson Prentice Hall, 2006. ISBN 9780131470897
- [21] Bagheria, S., Hadidi, A., Alilou, A. "Heightwise Distribution of Stiffness Ratio for Optimum Seismic Design of Steel Frames with Metallic-Yielding Dampers", *Procedia Engineering*, 14, pp. 2891–2898, 2011.  
<https://doi.org/10.1016/j.proeng.2011.07.364>
- [22] Ebadi Jamkhaneh, M., Ebrahimi, A. H., Shokri Amiri, M. "Experimental and Numerical Investigation of Steel Moment Resisting Frame with U-Shaped Metallic Yielding Damper", *International Journal of Steel Structures*, 19(3), pp. 806–818, 2019.  
<https://doi.org/10.1007/s13296-018-0166-z>
- [23] Maleki, S., Mahjoubi, S. "Dual-pipe damper", *Journal of Constructional Steel Research*, 85, pp. 81–91, 2013.  
<https://doi.org/10.1016/j.jcsr.2013.03.004>
- [24] Zheng, J., Li, A., Guo, T. "Analytical and experimental study on mild steel dampers with non-uniform vertical slits", *Earthquake Engineering and Engineering Vibration*, 14(1), pp. 111–123, 2015.  
<https://doi.org/10.1007/s11803-015-0010-9>
- [25] AISC "Specification for Structural Steel Buildings (AISC 360-16)", American Institute of Steel Construction, Chicago, IL, USA, 2016.
- [26] ATC "Improvement of nonlinear static seismic analysis procedures, FEMA-440", Applied Technology Council, Redwood City, CA, USA, ATC-55 Project, 2005.